

# MICROMECHANICAL ASPECTS OF THE INTER-FIBRE FAILURE IN FIBROUS COMPOSITE MATERIALS UNDER BI-DIMENSIONAL LOADS

París, F., Correa, E., Cañas, J. and Mantič, V.

School of Engineering, University of Seville, Camino de los Descubrimientos s/n, Sevilla, E-41092, Spain

## ABSTRACT

Many criteria have historically been proposed to predict failures in composites. Some of them were quasi-mimetically taken from metallic materials failure criteria and others were inspired by observation of the appearance of the failure of the composites. Prediction of the failure of the matrix (also called inter-fibre failure) has traditionally been assigned to a certain interaction (typically quadratic) between the components of the stress vector associated to the plane of failure. In this paper, a revision of these proposals is first of all carried out in order to examine in greater depth the implications of some of them. Then, a micromechanical study is conducted considering, based on failure observations, that the mechanism of failure starts with a crack running between fibre and matrix. The objective of this micromechanical analysis is to elucidate whether the assumption that the stress vector associated to a plane controls the failure of the plane is physically based. The numerical analysis is performed using the Boundary Element Method, allowing contact between the debonded surfaces of fibre and matrix. Different combinations of loads are applied (perpendicular and parallel to the plane of failure) to check their influence in the energy release rate, which is the fracture parameter evaluated. The results obtained prove numerically that stresses not associated to the macromechanical plane of failure play an important role in the micromechanism of failure of fibrous composites. This fact has been experimentally checked by means of the performance of a series of two dimensional loading tests.

## 1. INTRODUCTION

Although fibrous composite materials have traditionally been regarded as designed to work in the direction of the fibres, there are situations where the failure of the matrix (also called inter-fibre failure) plays an important role in the strength of the whole laminate or at least in a series of laminas of the laminate, such as, for example, the problem of an impact which generates stresses in all directions throughout the laminate.

Many of the existing proposals to predict this failure are variations of the original proposal by Hashin and Rotem [1] which basically estimates that the failure at one plane of the composite is governed by the components of the stress vector associated to this plane, a quadratic interaction between the components being additionally proposed. Thus, with reference to the failure of the matrix, they proposed Eqs. 1 and 2 for tension and compression respectively.

Matrix failure mode in tension:

$$\left(\frac{\sigma_{22}}{Y_T}\right)^2 + \left(\frac{\sigma_{12}}{S}\right)^2 = 1 \quad (1)$$

Matrix failure mode in compression:

$$\left(\frac{\sigma_{22}}{Y_c}\right)^2 + \left(\frac{\sigma_{12}}{S}\right)^2 = 1 \quad (2)$$

where:

$\sigma_{22}$  is the nominal stress in the lamina in the direction transversal to the fibres.

$\sigma_{12}$  is the nominal shear stress in the plane of the lamina.

$Y_T$  is the strength of the lamina in the direction transversal to the fibres in tension.

$Y_C$  idem in compression.

$S$  is the in-plane shear strength of the lamina.

As usual, axes 1 and 2 (1 coinciding with the orientation of the fibres) define the plane of the lamina. The above proposal of Hashin and Rotem had the unquestionable merit of distinguishing the mechanism of failure of fibrous composite materials, trying to propose criteria associated to them.

Hashin [2] tried to extend this idea to the three-dimensional case. Finding difficulties in determining the plane of failure, he assigned the failure to a quadratic interaction between stress invariants, cancelling in this expression the contribution of  $\sigma_{11}$ , based on the fact that any possible plane of failure is parallel to the fibres and that consequently, the components of the stress vector of any of these planes do not depend on  $\sigma_{11}$ . In the resulting criterion interactions between stresses and allowables, derived from the interactions between invariants, appear, not being clear what the consequences of this fact are. A wider study on this question can also be found in París [3] and in París et al [4].

Going back to the original idea of Hashin, there have recently been several proposals related with this idea. Taking as a reference an assumed plane of failure parallel to the fibres such as the one shown in Fig. 1, where the stress vector has three components,  $\sigma_n$ ,  $\tau_{nl}$ ,  $\tau_{nt}$ , (l represents the direction longitudinal to the fibres and t the transversal one), the original Hashin idea would have led to the following criterion:

$$\left(\frac{\sigma_n}{Y_C}\right)^2 + \left(\frac{\tau_{nl}}{S}\right)^2 + \left(\frac{\tau_{nt}}{S_T}\right)^2 = 1 \quad (3)$$

The main contribution to the inter-fibre failure based on this approach is Puck's theory known as 'action plane strength criteria'. This theory is explained in detail in Puck [5] and it is also covered in Puck and Schurmann [6], a paper presented in the context of a world wide failure exercise on fibrous composites. The theory is also presented by other authors, see for instance Kroll and Hufenbach [7] and Kopp and Michaeli [8].

Under tension ( $\sigma_n > 0$ ), the criterion is applied once the plane where the left hand side of Eq. 3 reaches a maximum is detected. In accordance with Puck's theory, 'generally the common strengths cannot be used in the denominators' of Eq. 3. Instead, they represent the resistances associated to the three components of the stress vector at the plane of failure.

Under compression ( $\sigma_n < 0$ ), the general idea is to alter Eq. 3 in order to allow it to predict the increase in strength of the lamina in presence of lateral compression. Thus, Eq. 4 is proposed.

$$\left(\frac{\tau_{nl}}{S - p_{nl}\sigma_n}\right)^2 + \left(\frac{\tau_{nt}}{S_T - p_{nt}\sigma_n}\right)^2 = 1 \quad (4)$$

Where  $p_{nl}$  y  $p_{nt}$  are material parameters associated to internal friction.

The two basic equations for tension, (3), and compression, (4), 'have been further modified to achieve a better agreement with experimental results', Puck and Schurmann [6], where the details of the modifications can be found.

Sun et al [9], in the context of a two-dimensional case, proposed a modification to the original quadratic interaction, in a similar manner to that described below. Thus, for the inter-fibre failure of a lamina, they proposed:

$$\left(\frac{\sigma_{22}}{Y}\right)^2 + \left(\frac{\tau_{12}}{S - \mu\sigma_{22}}\right)^2 = 1 \quad \text{with} \quad \mu = \begin{cases} \mu_0 & \sigma_{22} < 0 \\ 0 & \sigma_{22} > 0 \end{cases} \quad (5)$$

where  $Y=Y_T$  for  $\sigma_{22}>0$  and  $Y=Y_C$  for  $\sigma_{22} <0$  and where  $\mu$  is said to play a role similar to a friction coefficient.

Due to the fact that both proposals are firstly based on experimental macro-observations and on general reasoning (no support can be seen for the proposal at the level of the actual micromechanical failure) and secondly involve parameters that ought to be determined experimentally (basically using the proposed expression to adjust the value of the parameters), both could lead to accurate predictions. It is obvious that the two similar parameters ( $p$ 's and  $\mu$ ) would have different values, and that  $\mu$  ought to be greater than  $p$ 's to predict the failure at an equivalent level of nominal stresses.

The objective of this paper is to try to elucidate whether or not the main hypothesis of failure prediction of the matrix (i.e.: the failure at a plane is governed by the components of the stress vector associated to such a plane), which is the basis for the formerly presented approach, is a physically based assumption. To elucidate it negatively (i.e.: it is not a reasonable assumption) would make it nonsensical to discuss whether or not the quadratic interaction is reasonable.

To this formerly enunciated end a micromechanical analysis based on a boundary element model will be carried out. First, the micromechanical model, based on a unit cell with a single fibre partially cracked along the interphase, will be described, as well as the main features of the numerical analysis carried out. Then several loads will be applied on this model in one and two directions. The results obtained with the application of loads in two directions have motivated the development of a series of tests to try to support the conclusions obtained from the numerical results.

## 2. MICROMECHANICAL VIEW OF FAILURE

To be able to elucidate the stresses, and their interaction, involved in a mechanism of failure, the model to be developed has to consider the mechanism of failure of the material in question. In this case (failure of the matrix), it is considered, based on observations of damaged specimens such as that represented in Fig. 2, Gamstedt [10], that the damage starts at micromechanical level by a crack running circumferentially between the fibres and the matrix.

After these cracks have grown to a certain length, they interact with each other, giving rise to a macro-failure of the composite. The first step described, the growth of the crack between the fibre and the matrix, is the mechanism considered in this study. It is thought that this is the most significant period of generation of damage in an actual composite.

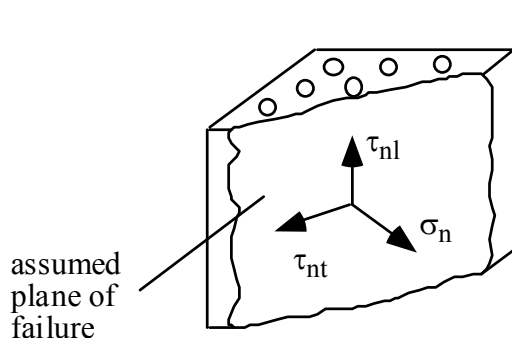


**Fig. 1.** Components of the stress vector in the assumed plane of failure.

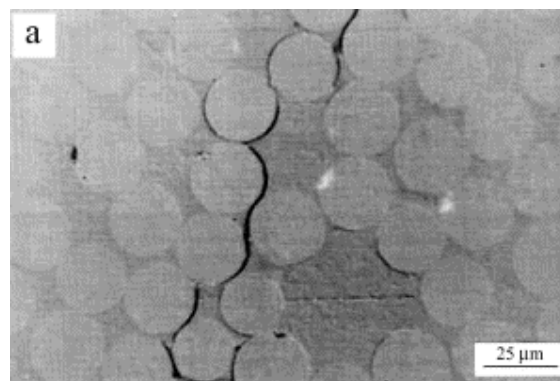


**Fig. 2.** Matrix/inter-fibre failure.

Fig. 3 represents the former explanations graphically. In Fig. 3a the failure at a plane in an idealized configuration of a fibrous composite is presented, a failure along a vertical plane being assumed in this case. This failure at micromechanical level involves, as the most

plausible mechanism of failure, the presence of a crack running between the fibre and the matrix as is indicated in Fig. 3b.

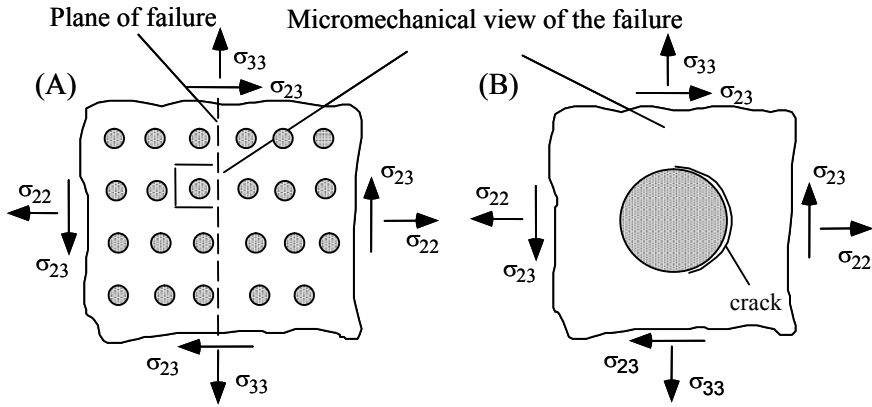


Fig. 3. Micromechanical scheme of the failure.

Initially a transversal section of an isolated fibre embedded in a matrix with an existing partial debonding between the fibre and the matrix in a plane strain state under remote stresses is going to be studied. This geometry, as deduced from Fig. 3, would lead in an actual composite when the damage is extensive and coalescence between the cracks arises, to a macro-failure along the vertical plane.

The question under consideration in this paper, with the model represented in Fig. 3, will make it possible to elucidate whether the components of the stresses that are not associated to the plane of failure (namely  $\sigma_{33}$  in Fig. 3b) play any role in the failure of the material (in this case, in the propagation of the crack).

## 2. THE BOUNDARY ELEMENT MODEL

The numerical analysis is going to be performed with the Boundary Element Method, Paris and Cañas [11], a similar configuration having already been studied by Paris et al [12]. The model permits the development of a contact zone ( $\theta_d$ - $\theta_s$  in Fig. 4) between the debonded surfaces of the fibre and the matrix to be taken into consideration. The two boundaries corresponding to the interface have been modelled in this study with continuous linear circular elements, those at both sides of the crack tip having discontinuous interpolation to facilitate the modelling of the possible singularities that will appear depending on the presence of contact zone along the debonded surfaces. The elements at both sides of the crack tip have a length of  $0.01745a$ ,  $a$  being the radius of the fibre. Details of the discretization performed can be found in [12].

To characterize the problem from the Fracture Mechanics point of view, the energy release rate will be used. The expression employed, in the crack closure technique, when the crack propagates from a certain angle  $\alpha$  to  $\alpha + \delta$  ( $\delta \ll \alpha$ ), is:

$$G_{\delta}^{arc}(\alpha) = \frac{1}{2\delta} \int_{\alpha}^{\alpha+\delta} \{(\sigma_{rr})_{\alpha}(u_r)_{\alpha+\delta} + (\sigma_{r\theta})_{\alpha}(u_{\theta})_{\alpha+\delta}\} d\theta \quad (6)$$

where  $\sigma_{rr}$  and  $\sigma_{r\theta}$  represent respectively radial and shear stresses along the interface and  $u_r$  and  $u_{\theta}$  their associated displacements. The two modes of fracture, I (associated to  $\sigma_{rr}$ ) and II (associated to  $\sigma_{r\theta}$ ), are obviously considered in this expression. The presence or not of contact zone between the debonded faces of matrix and fibre will in any case define the character of the mode of fracture. When the numerical model does not detect a contact zone (which happens for instance for a remote tension stress (in horizontal direction in Fig. 4) in presence of small debonding angles, smaller than 30 degrees (in the symmetric part solved), Paris et al

[12]), both stresses  $\sigma_r$  and  $\sigma_{r\theta}$  appear as singular in the model and the crack is working, in accordance with the numerical model developed, in a mixed mode. When a contact zone is detected, only  $\sigma_{r\theta}$  (with reference to the components of the stress vector ahead the crack tip) reaches a singular value, the crack then working in a pure shear mode. In absence of a significant contact zone the open model of interface fracture mechanics is applicable, Rice [13], whereas in presence of a significant contact zone the contact model, Comninou [14] is that applicable.

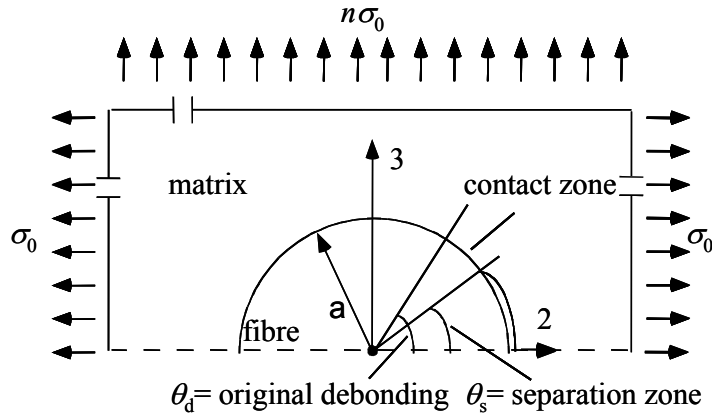


Fig. 4. Single fibre configuration.

The values of the energy release rate, for comparison purposes in the representations, will be normalized by means of:

$$\bar{G}(\theta_d) = G(\theta_d, \sigma_0) \frac{G^m}{a\sigma_0^2} \quad (7)$$

where  $G^m$  is the shear modulus of the matrix.

All the results have been obtained for a glass-epoxy system having the following properties:

$\nu^f$  = Poisson coefficient of the fibre = 0.22

$\nu^m$  = Poisson coefficient of the matrix = 0.33

$G^f$  = Shear modulus of the fibre =  $29 \cdot 10^9$  Pa

$G^m$  = Shear modulus of the matrix =  $1.05 \cdot 10^9$  Pa

$a$  = radius of the fibre =  $7.5 \cdot 10^{-6}$  m

## 4. NUMERICAL RESULTS

### 4.1. Energy release rate evolution

In this section loads in directions transversal and parallel to the assumed plane of failure are going to be considered as acting at the same time. The results of their simultaneous presence may differ significantly with respect to the case of acting independently due to the non-linear nature of the problem under consideration.

The values of the normalized energy release rate for several combinations of tension and compression in the two directions (normal and parallel to the plane of failure) are represented in Fig. 5, a deeper study of this matter appearing in París, et al [15]. In identifying the graphs, the first load corresponds to the horizontal direction and the second to the vertical direction (that in which the assumed plane of failure appears). To have a clear reference of the effect of the loads acting parallel to the plane of failure, the cases T-0 and C-0 (tension and compression normal to the plane of failure) are also included in the figure.

The results associated to the compression-compression case (C-C in Fig. 5) are, first of all, quite illustrative. The almost complete absence of released energy for this case of load is in absolute agreement with the well known fact (which inspired the modifications on failure of

the matrix in compression of Puck [5], Puck and Schürmann [6], Kroll and Hufenbach [7], Kopp and Michaeli [8] and Sun et al [9] already mentioned) that the failure of the matrix is delayed by the presence of iso-compression transversal to the fibres. It implies that the mechanism of failure for this configuration of load must be different to the one considered here but in any case it gives support to the significance of the micromechanical model developed. Debonding angles around 60° of have been proved to be the most adequate for the debonding cracks to suffer kinking, penetrating into the matrix, giving rise to the macrocrack sensibly normal to the applied load, París et al [16]

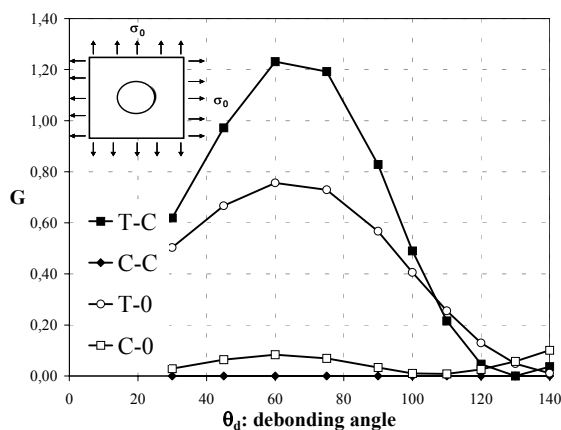


Fig. 5. Normalized energy release rate for bidimensional loads.

Analysing the remaining bi-dimensional case of load, this case of tension-compression (T-C in the figure) in relation to the simple application of a tension perpendicular to the plane of failure (T-0 in the figure), immediately attracts attention. The comparison of these two cases indicates the positive influence in the amount of released energy, within the range of debondings under consideration, of a compression parallel to the plane of failure superimposed on the traction nominally responsible for the failure.

As a conclusion of the studies carried out, represented by the results shown in Fig. 5, it is clear that in failures of the matrix controlled by the mechanism of failure modelled in this paper, it is not correct, from the model studied, to assign the failure at a certain plane to an interaction of the components of the stress vector associated to the plane of failure, it having been proved that the energy released during the failure is affected by the presence of components of the stress state not included in the stress vector.

Transferring the discussion to the case of a tension normal to the plane of failure, which is a case clearly associated to the mechanism of failure modelled here, the model developed predicts that the presence, for instance, of a compression parallel to the plane of failure of the same value as the nominal tension normal to the plane of failure, leads to the failure at a significantly lower value of this nominal tension (Fig. 5, T-0 and T-C cases for debonding angles around 60 degrees).

#### 4.2. Effect of the presence of friction

Some factors might affect the conclusions obtained above from the numerical results of the T-C case. In this section one of these factors, the presence of friction in the contact zone of the debonded part of fibre and matrix, is going to be studied. This effect could simulate the predictable not absolutely smooth nature of the debonded surfaces of fibre and matrix.

In order to evaluate the influence of the presence of friction in the problem, Fig. 6 shows the evolution of the normalized energy release rate  $G$  as a function of the debonding angle for

different values of the friction coefficient ( $\mu= 0, 0.1, 0.25, 0.5$ ) for the aforementioned T-C case. From the figure it can be observed that, though the tendency observed in the evolution of the energy release rate does not seem to remarkably change from that shown for the frictionless case, the values of the energy release rate decrease in absolute terms due to the presence of friction.

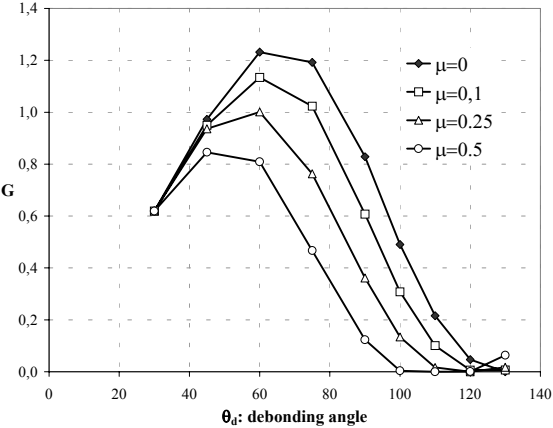


**Fig. 6.** Normalized energy release rate for the T-C case. Effect of friction.

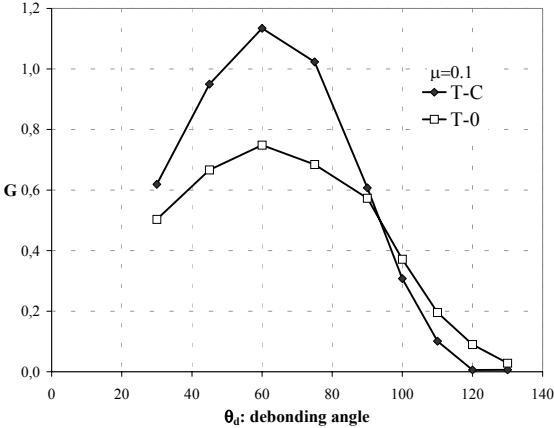


**Fig. 7.** Normalized energy release rate comparison between cases T-C and T-0 ( $\mu=0.1$ ).

This fact makes it necessary to compare the results obtained for the T-C case (in presence of friction) with the values of the T-0 case also in presence of friction, in order to check if the conclusion obtained in section 4.1 (i.e.: the positive influence in the amount of released energy, within the range of debondings under consideration, of a compression parallel to the plane of failure superimposed on the traction nominally responsible for the failure) is independent of the presence of friction. Thus, in Figs. 7, 8 and 9 the comparison between the T-C case and the T-0 case for different values of the friction coefficient ( $\mu= 0.1, 0.25, 0.5$ ) are shown. It can be observed from these figures that, though as  $\mu$  increases T-C and T-0 curves seem to get closer, higher values are always found for the T-C energy release rate than for the T-0 energy release rate for the range of debondings of interest, less than  $60^\circ$ . As a summary, the maxima of the ratio of the energy release rate for the T-C case to the T-0 case appear in Table 1 for the different values of coefficient  $\mu$  considered, also including the debonding angle at which the corresponding maximum takes place.

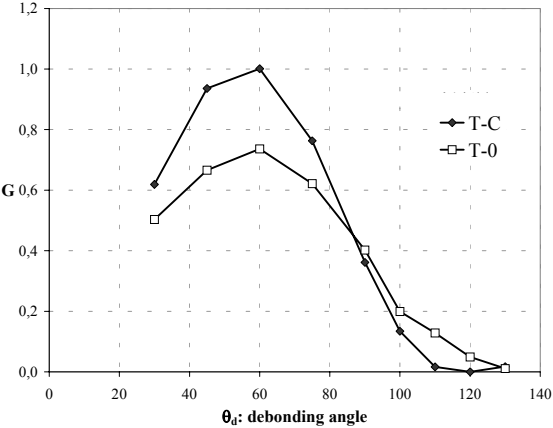


**Fig. 8.** Normalized energy release rate comparison between cases T-C and T-0 ( $\mu=0.25$ ).

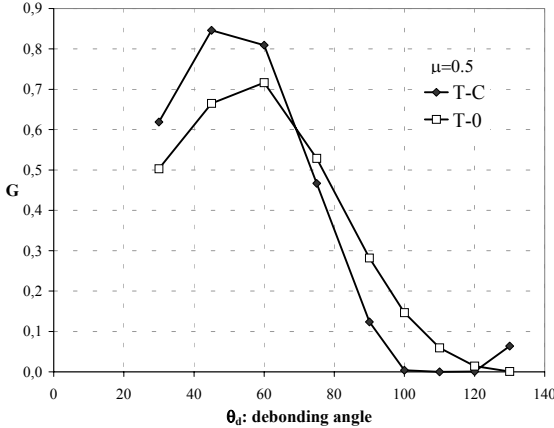


**Fig. 9.** Normalized energy release rate comparison between cases T-C and T-0 ( $\mu=0.5$ ).

**Table 1.** Summarized results of the effect of friction.

	$\mu=0$	$\mu=0.1$	$\mu=0.25$	$\mu=0.5$
$G^{T-C}/G^{T-0})_{\max}$	1,63	1,51	1,36	1,61
$\theta$ (°)	60	60	60	45

## 5. EXPERIMENTAL STUDY

In order to check the correspondence between the numerical predictions formerly obtained and the behaviour of an actual composite under a situation similar to any of those considered in the paper, some appropriate experiments have been carried out.

In selecting the test, the lack of a standard two-dimensional test and its corresponding device is the first problem. The existing two-dimensional machines are thought to apply the loads in the plane of the lamina, but in the case under consideration in this paper, one of the loads has to be applied perpendicular to the plane of the lamina. The simplest scheme of application of the required two-dimensional loading is to select the tension applied by the universal test machine as the load leading to the failure and to apply additionally transversal compression to the lamina. An additional advantage of selecting this configuration is that the differences in the maximum values of the energy release rate corresponding to this case and those corresponding to the simple application of a longitudinal tension are quite significant (see cases T-0 and T-C in Fig. 5). Thus, if the starting of damage is controlled by the assumed mechanism and this period of debonding between fibres and matrix is dominant (in terms of the total energy absorbed by the material), versus the period of coalescence of these debondings to generate a macrocrack, the effect in testing of the response of the material to the presence of a lateral pre-compression ought also to be quite significant.

Although in the numerical study carried out the two loads are applied simultaneously, in performing the test the lateral compression has been applied first (we will refer to it as pre-compression in what follows) and then is maintained while tension is applied until the breakage of the specimen. Thus, the test corresponds to the conventional 90 degrees test in tension (performed in accordance with standard ASTM D-3039M) with a lateral transversal pre-compression applied. The width of the specimens has been altered with respect to that indicated in the standard in order to allow the application of the lateral load.

When comparing the experimental results with the numerical predictions it is important to notice that although the application of the two loads in the numerical modelling is simultaneous, whereas it is sequential in the testing, this fact does not alter the degree of comparison of both results. This is correct because in the numerical modelling, and in absence of friction, the results, since the problem is a conforming contact problem, are independent of the order of application of the loads.

Fig. 10 represents pictures of the machine while running a test. The material tested being a graphite-epoxy denominated Z-19.775. Specimens of three different thicknesses (corresponding to 8, 12 and 16 plies) have been tested, no influence of this thickness having been found on the results.

With reference to the final breakage of the specimen the vast majority of them do so throughout a horizontal plane (transversal to the tension applied) placed inside the zone of application of the lateral pre-compression, a fact that proves the implication of the biaxial state of load applied in the final mechanism of failure and eliminates the effect of the local singular compression stress induced by the lateral punch into the specimen at the corner of the punch.

To evaluate the effect of the application of the lateral pre-compression, the results thus obtained will be compared with those obtained with the simple application of a tension longitudinal with the specimen (transversal to the fibres). Thus, the cases denominated by T-0 and T-C, whose results appear in Fig. 5, will be those under comparison.



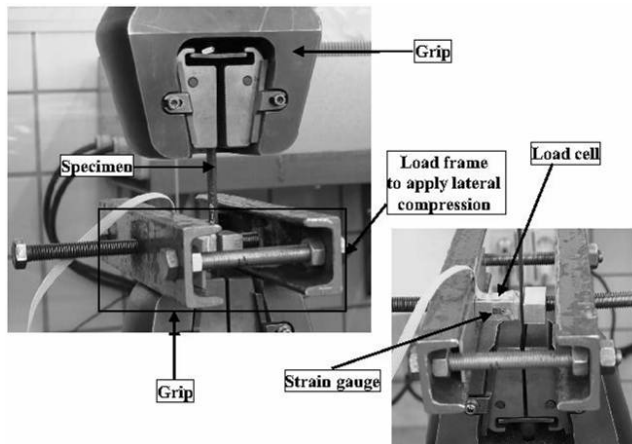


Fig. 10. Bi-dimensional test running.

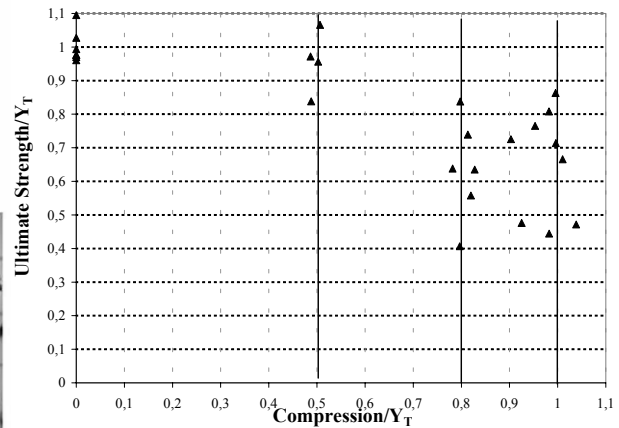


Fig. 11. Bi-dimensional test results.

Three levels of lateral pre-compression have been nominally applied:  $0.5 Y_T$ ,  $0.8 Y_T$  and  $Y_T$ ,  $Y_T$  being the rupture stress in testing the specimen in tension without lateral pre-compression. Due to the fact that the lateral pre-compression is applied manually by means of a screw system of a different degree of accuracy than the vertical load, some of the cases do not correspond exactly to the nominal loads formerly indicated. This will be appreciated in the representation of the results. It has been judged preferable to try to maintain the same indications for the two strain gauges rather than to apply exactly the nominal lateral value of the compression, which in fact has no significant influence in the question under consideration. In any case, the situations of maximum interest are obviously those where the value of the lateral pre-compression load is in the neighbourhood of  $Y_T$ .

The results are summarized in Fig. 11. The ratio of the ultimate strength of each specimen with lateral pre-compression to  $Y_T$  versus the ratio of lateral pre-compression to  $Y_T$  is represented for the different specimens tested. The results share the typical level of scattering found in fibrous composite materials when they are tested perpendicularly to the fibres. Nevertheless, the general tendency observed is in complete agreement with the behaviour predicted by means of the numerical analysis previously carried out. Thus, the application of a lateral pre-compression parallel to the assumed plane of failure produces a significant reduction in the longitudinal tension that produces the rupture of the specimen. This rupture tension load is consequently a function of the lateral pre-compression applied. This fact, in conjunction with the appearance of a horizontal plane of failure to which the lateral compression is not associated as a component of the stress vector, supports the idea that the components of the stress vector associated to a plane may not be enough to predict the failure of the plane.

## 7. CONCLUSIONS

Fundamentals of criteria associated to predictions of failure of the matrix in fibrous composite materials have been revised by means of a micromechanical numerical boundary elements model complemented by the performance of suitable tests.

It has been shown that to associate the failure of the matrix at a plane to a certain interaction between the components of the stress vector associated to the plane does not, generally speaking, appear to be a physically based hypothesis. This fact has been proved assuming, based on experimental observations, that the mechanism of failure is associated to cracks running between fibre and matrix and interacting between them to create a zone of damage of macromechanical meaning. It has been shown that the presence of a compression parallel to the plane of failure accompanying the nominal tension responsible for the failure significantly

affects the amount of energy released by a crack running circumferentially between fibre and matrix. This has been exactly the situation considered in the experiments carried out, which have supported the predictions deduced from the numerical analysis. The influence of this normal stress parallel to the plane of failure in the inter-fibre failure of the composite is not covered by the criteria which only include the components of the stress vector associated to the plane of failure. Additionally, the influence of the presence of friction in the problem under consideration has been checked, founding that, though the values of the energy release rate change quantitatively, this fact does not alter the conclusions obtained for the frictionless case.

In the former conclusions, it has obviously been assumed that the growth of the crack between the fibre and matrix is the major representative mechanism in the formation of damage at macromechanical level, the released energy in connecting the interface cracks associated to different fibres not being representative for a real composite material with a significant fibre volume fraction.

## References

1. **Hashin, Z.** and **Rotem, A.**, "A fatigue failure criterion for fiber reinforced materials", *J. Composite Mats.*, **7** (1973), 448-464.
2. **Hashin, Z.**, "Failure criteria for unidirectional fiber composites", *J. App. Mech.*; **47** (1980), 329-334.
3. **París, F.**, "A study of failure criteria of fibrous composites materials". *NASA/CR-2001-210661*, (2001).
4. **París, F., Marín, J. C.** and **Cañas, J.** "A discussion on Hashin proposals on failure of the matrix in compression". In: ECCM9, Composites-from fundamentals to exploitation, *ESCM, Brighton (UK)*, (2000).
5. **Puck, A.**, "Festigkeitanalyse von Faser-Matrix-Laminaten, Modelle für die Praxis (Strength analysis of fibre-matrix/laminates, models for design practice)", *Carl Hanser Verlag*, Munich, Germany (1996).
6. **Puck, A.** and **Schürmann, H.**, "Failure analysis of FRP laminates by means of physically based phenomenological models", *Comp. Sci. Tech.*, **58** (1998), 1045-1067.
7. **Kroll, L.** and **Hufenbach, W.** "Physically based failure criterion for dimensioning of thick-walled laminates", *App. Comp. Mat.*, **4** (1997), 321-332.
8. **Kopp, J.** and **Michaeli, W.**, "Dimensioning of thick laminates using new IFF strength criteria and some experiments for their verification", *Proceedings of the ESA ESTEC Conference* (1996); 305-312.
9. **Sun, C. T., Quinn, B. J., Tao, J.** and **Oplinger, D. W.**, "Comparative evaluation of failure analysis methods for composite laminates", *DOT/FAA/AR-95/109* (1996).
10. **Gamstedt, E. K.**, "Fatigue Damage Mechanisms in Polymer Matrix Composites", *PhD Thesis*, Lulea Univ. of Technology (1997).
11. **París, F.** and **Cañas, J.**, "Boundary Element Method. Fundamentals and Applications", *OUP* (1997).
12. **París, F., del Caño, J. C.** and **Varna, J.**, "The fiber-matrix interface crack.- A numerical analysis using Boundary Elements", *Int. J. Fract.*, **82/1** (1996), 11-29.
13. **Rice, J. R.**, "Elastic fracture mechanics concepts for interfacial cracks", *J. Appl. Mech.*, **55** (1988), 98-103.
14. **Comninou, M.**, "The interface crack", *J. Appl. Mech.*, **44** (1977), 631-636.
15. **París, F., Correa, E.** and **Cañas, J.**, "Micromechanical view of failure of the matrix in fibrous composite materials", *Comp. Sci. and Tech.*, **63** (2003), 1041-1052.
16. **París, F., Correa, E.** and **Mantič, V.**, "Study of kinking in transversal interface cracks between fibre and matrix", In: ECCM-10, Composites for the future, *ESCM, Brugge (Belgium)*, (2002).